Physicochem. Probl. Miner. Process., 58(4), 2022, 149673

http://www.journalssystem.com/ppmp

Physicochemical Problems of Mineral Processing

ISSN 1643-1049

Enhanced effect of fine magnetite on the flotation performance of fine hematite in sodium oleate system

Bin Pei [1], Ximei Luo [1,2], Wen Yang [1], Dayong Wei [1,2], Chao Li [1], Yunfan Wang [2,3]

[1] Faculty of Land and Resource Engineering, Kunming University of Science and Technology, Kunming 650093, China

[2] State Key Laboratory of Complex Nonferrous Metal Resources Clean Utilization, Kunming University of Science and Technology, Kunming 650093, China

[3] Faculty of Metallurgical and Energy Engineering, Kunming University of Science and Technology, Kunming 650093, China

Corresponding authors: 85128225@163.com (Ximei Luo), asc_cloud@aliyun.com (Yunfan Wang)

Abstract: In this work, the effect of magnetite with different particle sizes on the flotation performance of both coarse and fine hematite particles were investigated by using sodium oleate as a collector. The results showed that the magnetite particles with different particle sizes showed a negative effect on hematite (-106+45 μm) recovery, but the addition of magnetite with the same particle sizes as hematite during the direct flotation of -45 μm hematite was beneficial to improve the recovery of micro-fine hematite and the Fe grade of concentrate. The finer the magnetite particle was, the more obvious the agglomeration effect of hematite was. Therefore, the beneficial effect could be achieved by adjusting the particle sizes of particles. Moreover, sodium oleate was beneficial to promote the agglomeration of micro-fine magnetite and hematite. The results from the microscopic analysis, laser particle size analysis, and EDLVO calculation proved that there was an effective aggregation between fine magnetite and fine hematite particles, which increased the apparent size of hematite particles and the probability of the mineral particles adhering to bubbles, thus improving the hematite recovery.

Keywords: magnetite, hematite, flotation, magnetic aggregation

1. Introduction

With the depletion of high-grade iron ore resources, more effective mineral separation techniques for medium-grade and low-grade iron ores are required. The properties of refractory iron ores are relatively complex because of the close association and fine dissemination between valuable minerals and gangues. The valuable minerals can be liberated from the gangues after the "run-of-mine" ores are ultra-finely comminuted firstly (Hu et al., 2013; Bode et al., 2020). However, it will cause extreme sliming of ores which makes different minerals cover each other, and further affect the floatability of the valuable minerals. As a result, the discrepancy between minerals and gangues in flotation will be reduced, and the adhesion efficiency between mineral particles and bubbles will be lowered as well, resulting in extreme difficulty in separating valuable minerals from gangues (Paiva and Rubio, 2016; Zhuo et al., 2018; Darabi et al., 2020).

In order to enhance the flotation efficiency of fine particles, many methods such as hydrophobic (shear) flocculation and selective flocculation have been studied (Panda et al., 2011; Ozkan and Duzyol, 2014; Li et al., 2018; Ma et al., 2019; Hao et al., 2019). The flocculation-flotation method has predominant advantages for separating fine-sized minerals (Forbes, 2011; Forbes et al., 2019). The fine-sized minerals can be polymerized or flocculated after adding appropriate amounts of flocculants, and the apparent size of particles increases, resulting in the distinct discrepancy of sorting and the high collision probability between bubbles and particles. In recent years, the challenge, faced by mineral processors, is that the flotation indexes of fine hematite ores are poor (Pascoe and Doherty, 1997; Chapman et al., 2011; Rao et al., 2013). Researchers have tried to solve this problem by increasing the dosage of flotation reagents and using highly selective flocculants (Luo et al., 2016; Li et al., 2018; Fu et al., 2018). To some

DOI: 10.37190/ppmp/149673

extent, these methods have received effective effects, but the disadvantages should also be taken into account: the consumption of flotation reagents and the cost of recycling is high. Therefore, more effective solutions need to be explored.

Fundamentally, the flocculation flotation technology is aimed at enlarging the apparent diameter of fine particles to an appropriate size by adsorption, consequently promoting flotation efficiency. It is reported that magnetic aggregation technology can remove heavy metal ions from wastewater and reduce its turbidity (Ahmed et al., 2013; Akinwekomi et al., 2020). Magnetic force can also gather weakly magnetic mineral particles and magnetite particles together. Just like adding flocculants, the effect of increasing the apparent diameter can be achieved. The application of "magnetic aggregation" in mineral processing can not only reduce the consumption of flotation reagents but also improve the flotation efficiency (Li et al., 2017; Yin et al.,2019; Yue et al., 2019). There are also some studies (Pindred and Meech, 1984; Li et al., 2019) that have shown that it is not necessary to add magnetite, hematite particles are more than adequate to collect fine hematite particles. However, only when the content of coarse particles is appropriate, can the coarse particles have a self-carrier effect in the flotation process. Excessive coarse particles will weaken this strengthening effect, resulting in part of fine hematite particles cannot being recovered.

In this work, the effect of magnetite with different particle sizes on the flotation performance of coarse and fine hematite particles was investigated using sodium oleate as a collector. The sedimentation tests, microscopic analysis, and laser particle size analysis were utilized to reveal the mechanism of enhancing the effect of fine magnetite on the flotation performance of fine hematite particles.

2. Materials and methods

2.1. Materials

The pure minerals used in the test were hematite and magnetite samples which were carefully handpicked, crushed, ground, and then purified by gravity and magnetic separation. Subsequently, the products were wet sieved to obtain particle size fractions in the range of -106+45 μm, -45 μm, -45+18 μm, and -18 μm, which were employed for the tests. The XRD patterns of the two pure minerals are shown in Fig. 1 and the results of the chemical analysis are shown in Tables 1 and 2, respectively. X-ray diffraction analysis and chemical analysis of the two samples show that the purity of magnetite and hematite was higher than 96%.

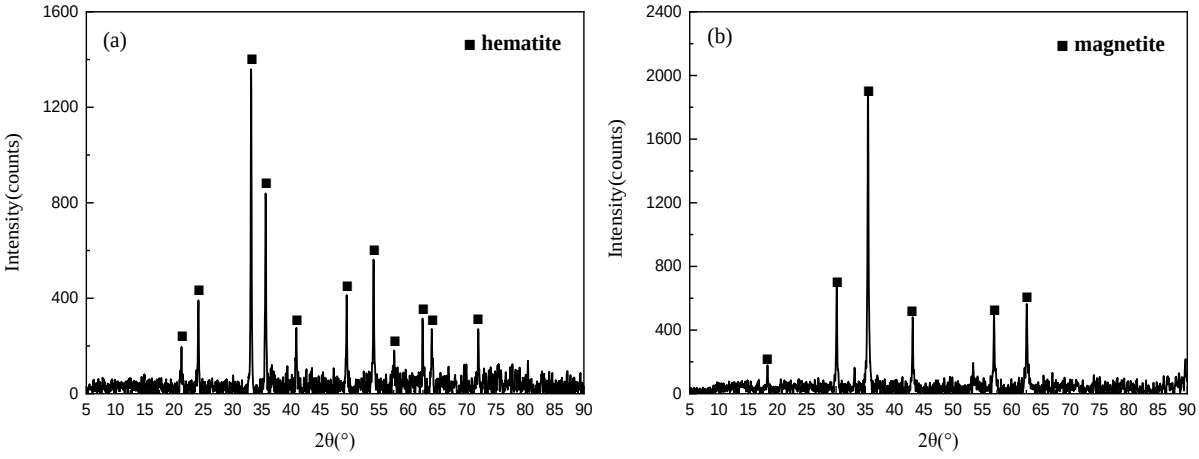

Fig. 1. X-ray diffraction spectrum of (a) hematite and (b)magnetite

Table 1. Chemical element analysis of hematite sample

Constituents	TFe	FeO	SiO_2	Al_2O_3	MgO	CaO	P	S
Contents (%)	69.20	< 0.15	0.55	0.33	0.0027	0.000659	0.11	0.00027

Table 2. Chemical element analysis of magnetite sample

Constituents	TFe	FeO	SiO_2	Al_2O_3	MgO	CaO	P	S
Contents (%)	70.30	28.65	0.24	0.26	1.72	0.00027	0.000658	0.082

2.2. Reagents

Sodium oleate and sodium hydroxide (NaOH) with more than 98% purity were obtained from different chemical companies in China. Sodium oleate was adopted as the anionic collector, and NaOH was used as a pH regulator. Deionized (DI) water was employed in all experiments.

2.3. Methods

2.3.1. Micro-flotation experiments

Pure mineral flotation experiments were carried out in a 30 cm^3 XFG flotation cell with the impeller speed of 1500 rpm at room temperature. During each flotation experiment, 2 g of samples composed of magnetite and hematite in different proportions by weight according to test design, mixed with 25 cm^3 DI water, was added into the flotation cell with a mechanical agitation for 1 min. Then, the pH value was regulated with NaOH, and the collector was added to the suspension in sequence. The pulp was conditioned for 2 min with each reagent. The flotation time was fixed for 3 min. After the flotation experiments, the foam and sink products were collected, filtered, dried, weighed, and analyzed. Each flotation test was performed at least three times. Both the average and standard deviation values were recorded. It is worth noting that since both magnetite and hematite contain Fe, to investigate the effect of magnetite on hematite recovery, total iron recovery, magnetite recovery, and hematite recovery were obtained from chemical element analysis of TFe and FeO.

2.3.2. Sedimentation tests

The aggregation behavior between fine magnetite particles and fine hematite particles was investigated by sedimentation tests (Medvedeva et al., 2013). Quantitative hematite particles were mixed with 100 cm^3 DI water in a beaker for 3 min. Magnetite particles with different particle sizes and the pH regulator (NaOH) were separately added. The pH value was adjusted to approximately 9. Then, the suspension was stirred for 3 min. The settling time of agglomerates was calculated by the STOKES formula. After standing, the supernatant (slime) with a height of 10 cm was discharged, and the rest (M) was the settling sand. Afterward, the sand products were collected, filtered, dried, weighed, and analyzed. The sedimentation rate is calculated using Eq. 1:

$$\text{Sedimentation Rate} = \frac{M}{M_0} \times 100\% \tag{1}$$

where M is the quality of minerals in sand products; M_0 is the total mass of minerals (hematite and magnetite added).

2.3.3. Microscopic analysis

The interaction between fine magnetite particles and fine hematite particles was analyzed by a high-speed camera. Their dynamic behavior and flocculation morphology were analyzed.

2.3.3.1. Dynamic behavior

The hematite particles (-45 μm) were adsorbed with the resin glue on the silver needle (φ=120 μm) surface. Afterward, about 10 cm^3 of DI water with a fixed pH value was injected into a transparent organic cell, and the sodium oleate (240 mg/dm^3) was added in advance as required. The silver needle with hematite particles was then fixed in the centre of the organic cell, and the part of the silver needle covered by hematite particles was submerged in the DI water. Subsequently, the slurry containing magnetite particles was added to this organic cell. Simultaneously, the black and white high-speed camera was used for shooting and timing. The photos were taken at 0 sec, 2.5 min, and 5 min, respectively.

2.3.3.2. Flocculation morphology

First, the hematite particles (-45 μm) were added to the organic cell, and then distilled water, reagents, and magnetite particles were separately added according to the test design. The solution with distilled water, reagents, and particles was quickly stirred, and 1-2 drops were evenly extracted on the freshly stripped mica with a pipette, and then the mica sheet was observed and analyzed by a microscope. Mica was chosen because of its strong hydrophilicity, on which the liquid could spread out instantly to ensure that the particles did not overlap with each other. The structure diagram of the microscope and relevant equipment is shown in Fig. 2.

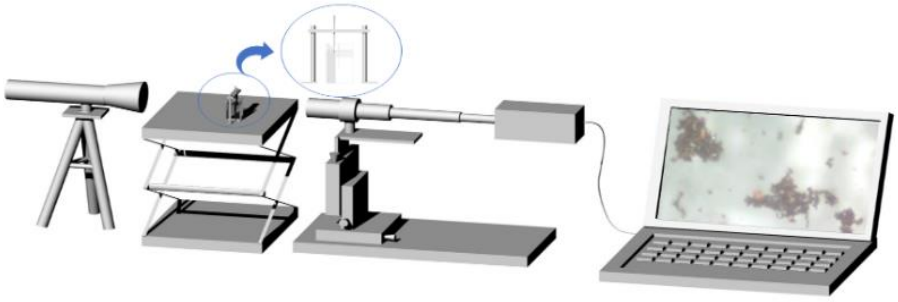

Fig. 2. Microscopic equipment diagram

2.3.4. Laser particle size analysis

The laser particle size analyzer is used to measure the size of solid particles in terms of the scattering phenomenon of light (Syvitski, 1991; Haselhuhn and Kawatra, 2015). The fine-sized particles have larger scattering angles; while the coarse particles have smaller scattering angles. The intensity of scattering is also related to particle size. On the one hand, the coarse particles will produce the scattering light with narrow-angle and high intensity, while the fine particles will generate the scattering light with wide-angle and low intensity. Meanwhile, the intensity reduces as the particle volume decreases. The laser particle size analyzer (Mastersize 2000) was used in the tests.

3. Results and discussion

3.1. Micro-flotation experiments

Fig. 3 shows the effect of magnetite with different particle sizes on the flotation of hematite with the particle size of -106+45 μm (coarse-grained hematite) using sodium oleate with a concentration of 120 mg/dm^3 at pH=9. As shown in Fig. 3, the Fe grade of concentrate slightly increased after adding magnetite particles with different particle sizes, but the recovery of the coarse-grained hematite was reduced to some extent, which showed a negative effect on the direct flotation of coarse-grained hematite. However, the negative effect of magnetite with different particle sizes on hematite was different. The effect order of magnetite with different particle sizes on the coarse-grained hematite recovery was displayed as follows: -45+18 μm magnetite > 18 μm magnetite > -106+45 μm magnetite (almost no effect). The addition of magnetite with a particle size of -45 μm significantly reduced the coarse-grained hematite recovery, while the magnetite with the particle size of -106+45 μm had the least effect. Additionally, it was found that when -18 μm magnetite particles were added, the foam was rich and stable. The experiment showed that adding fine particles was beneficial to increasing the number and stability of bubbles, and fine particles acted as a kind of "foaming agent". Vieira and Peres (2007) pointed out that the presence of a certain amount of fine particles in pulp could affect the shape of bubbles, reduce the size of bubbles and improve their stability of bubbles. Leja (1956, 1957) discussed the effect of solid particles entering the foam structure on foam stability, pointing out that the hydrophobic solid particles were firmly bound together as they could enter the air/water interface, limiting the outflow of liquid and thus improving bubble stability. According to this theory, due to the larger specific surface area of fine magnetite particles, more collectors would be absorbed, and a higher hydrophobic degree would be achieved, which was more conducive to the stability of the foam.

Therefore, it is the reason why the hematite recovery after adding magnetite (-18 μm) is higher than that after adding magnetite (-45+18 μm).

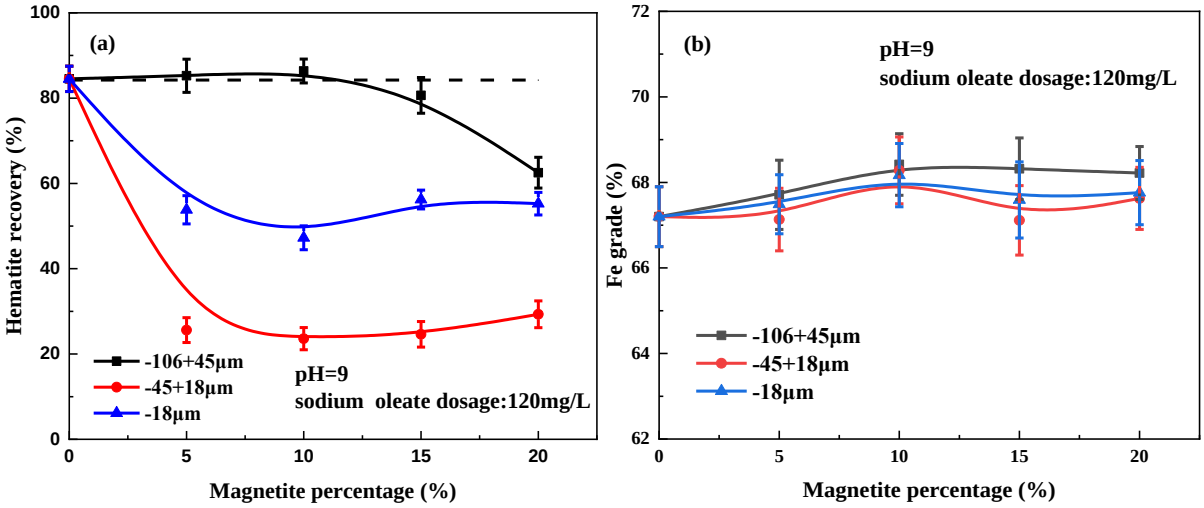

Fig. 3. Effect of magnetite on hematite (-106+45 μm) recovery (a) and Fe grade (b) in concentrate

Fig. 4 indicates the effect of magnetite with different particle sizes on the flotation of hematite with the particle size of -45 μm (fine-grained hematite) using sodium oleate with a concentration of 240 mg/dm^3 at pH=9. Figure 4 shows that in the direct flotation of fine-grained hematite (-45 μm), the addition of the magnetite particles with the same particle sizes as hematite was beneficial to improving the Fe grade and recovery of concentrate, but the addition of magnetite with different particle sizes (-106+45 μm) as hematite would reduce the flotation recovery of hematite (-45 μm). Therefore, based on the effect above, the beneficial effect can be achieved by adjusting the particle sizes to avoid the adverse effect.

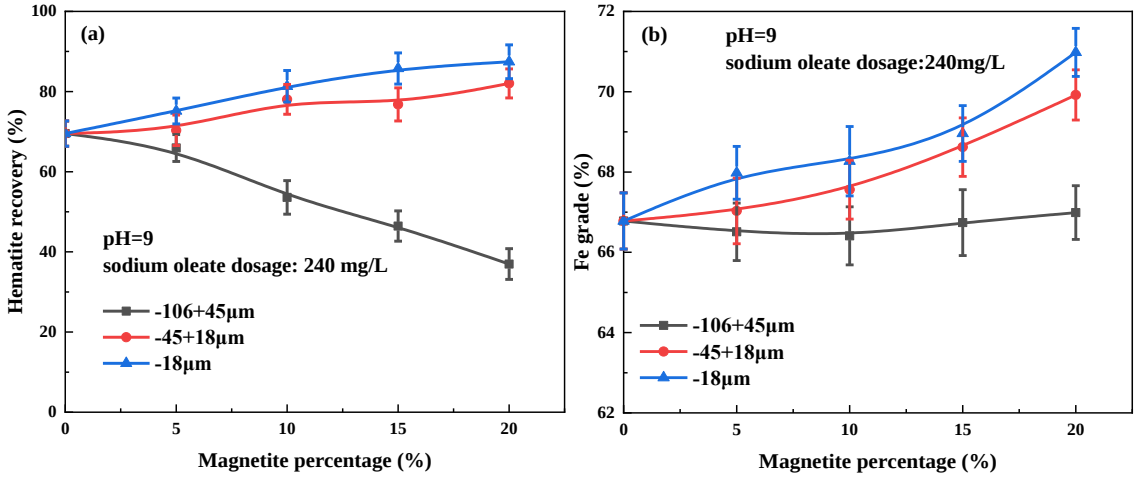

Fig. 4. Effect of magnetite on hematite (-45 μm) (a) recovery and (b) Fe grade in concentrate

3.2. Microscopic analysis

3.2.1. Dynamic behavior

Fig. 5 manifests the microscopic images of hematite in distilled water before and after adding fine magnetite particles at pH=9 for different periods. As shown in Fig. 5, a few fine magnetite particles appeared on the surface of fine hematite after adding magnetite particles at 2.5 min, indicating that there was an interaction between the fine hematite and the fine magnetite particles without any reagent. After adding magnetite particles for 5 min, a large number of fibrous clumps appeared on the surface of the hematite, manifesting that the flocculation effect between fine magnetite and fine hematite was more

obvious with the increase of time. The reason for this phenomenon might be that fine magnetite particles had a certain natural magnetism, especially when the particle size was reduced to about -10 μm (Wang and Forssberg, 1992), a higher magnetic gradient effect would occur (Schaller et al., 2008). In this way, the magnetic force acting on the surrounding hematite particles increased sharply, resulting in magnetic aggregation. The fine magnetite particles acted as a "steel wool" medium in a high gradient magnetic separator (Zhang et al., 1986). The antiferromagnetism of hematite and the corresponding change of magnetism was the internal reason why hematite could be agglomerated by magnetite particles (Robinson et al., 2004; Bhowmik and Saravanan, 2010).

Fig. 6 displays microscopic images of hematite in sodium oleate solution before and after adding fine magnetite particles at pH=9. As shown in Fig. 6, the surface of fine hematite was also covered with whisker flocs of magnetite after adding fine magnetite particles at 2.5 min in the sodium oleate system. Furthermore, after adding magnetite particles for 5 min, a large number of fibrous flocs appeared on the surface. It also indicated that there was flocculation between fine magnetite and fine hematite in the sodium oleate system. Additionally, it could be seen from Fig. 6 that the flocs on the hematite surface after adding sodium oleate were more than that without adding sodium oleate at the same time, which indicated that sodium oleate could promote the aggregation between magnetite and hematite particles. These results demonstrated that the interaction between the fine magnetite and hematite particles could produce an aggregation effect and increase the apparent size of fine hematite particles at pH 9. On the other hand, sodium oleate played an important role in promoting the aggregation of fine hematite particles.

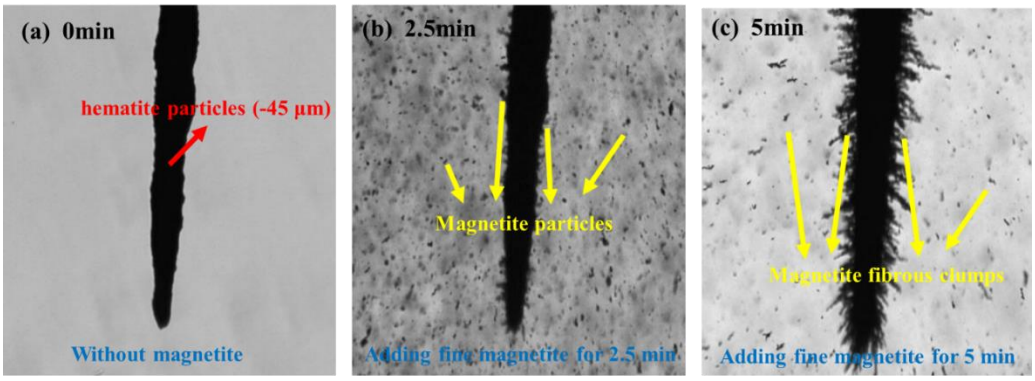

Fig. 5. Flocculation of hematite (-45 μm) before and after adding fine magnetite (-18 μm) at pH=9

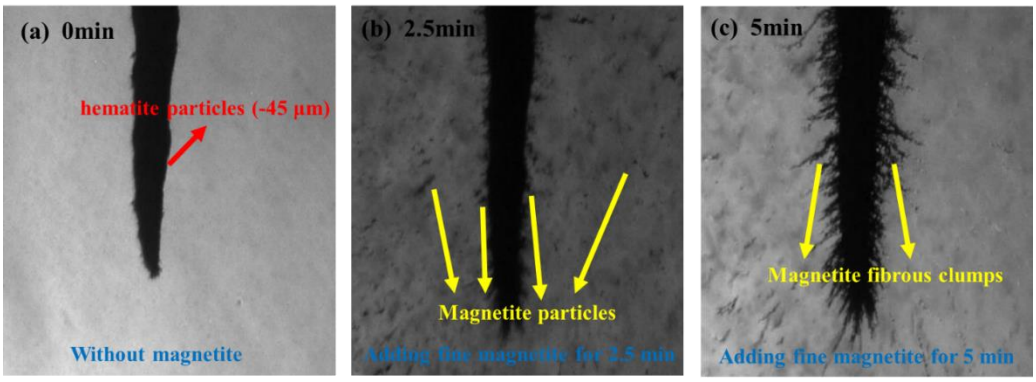

Fig. 6. Flocculation of hematite (-45 μm) and fine magnetite (-18 μm) in sodium oleate solution (240 mg/dm^3) at pH=9

3.2.2. Flocculation morphology

The microscopic images of hematite in sodium oleate solution at pH=9 before and after adding fine magnetite particles are shown in Fig. 7. According to the results in Fig. 7, the hematite and magnetite particles formed flocs with larger particle sizes in the sodium oleate system such as granular flocs and

whisker flocs. This proved that the fine magnetite and the fine hematite agglomerated effectively in the sodium oleate system.

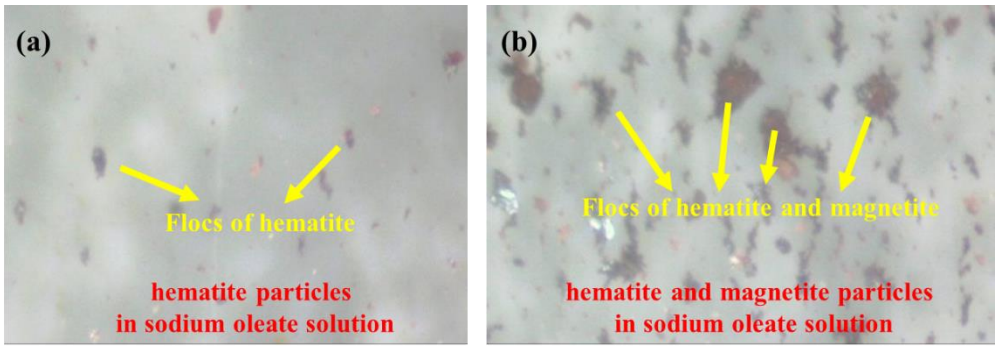

Fig. 7. Flocculation of hematite and fine magnetite before and after their interaction in sodium oleate solution (pH=9) red particles—hematite, black particles—magnetite

3.3. EDLVO calculation

The extended DLVO (EDLVO) theory, which accounts for not only the electrostatic interaction and van der Waals force, but also other effects such as the polar interfacial interaction, hydrophobic interaction, and so on, can explain the hydrophobic aggregation of particles under a certain condition (Li et al., 2017). In the dispersion and stability system of particles, there are at least the following kinds of interaction energy (Guo et al., 1999; Hu et al., 2020): electrostatic energy (V_R), Van Der Waals interaction energy (V_A), magnetic energy (V_{MA}) and hydrophobic energy (V_{HA}). Therefore, the total energy (V_T^{ED}) of the interaction between particles can be calculated by Eq. 2:

$$V_T^{ED} = V_R + V_A + V_{MA} + V_{HA} \tag{2}$$

3.3.1. Electrostatic energy (V_R)

The electrostatic interaction energy is the mutual effect energy between the particle surfaces of magnetite and hematite in the diffusion layer with the different or same charge ions to attract or repel each other. Considering that the surface potential of magnetite in slurry has been fixed, the electrostatic interaction energy (V_R) between spherical particles is calculated by Hogg's proposed method:

$$V_R = \frac{\pi\varepsilon_0\varepsilon_r R_M R_H(\phi_{M1}^2+\phi_H^2)}{R_M+R_H}\left\{\frac{2\phi_M\phi_H}{\phi_M^2+\phi_H^2} In\left[\frac{1+e^{(-kH)}}{1-e^{(-kH)}}\right] + In\left(1-e^{(-2kH)}\right)\right\} \tag{3}$$

where R_M and R_H are the particle radius of magnetite and hematite; ε_0 is the vacuum dielectric constant; ε_r is the relative dielectric constant; ϕ_M and ϕ_H are magnetite and hematite surface potentials; K is the Baideye-Heckel constant; X is the distance between magnetite and hematite.

The information required for calculation is exhibited as follows: the average diameter of hematite was 26.15 μm; the average size of magnetite particles was 32 μm, 13.14 μm, and 7.2 μm; $R_{M1} = 3.2\times10^{-5}$ m, $R_{M2} = 1.314\times10^{-5}$ m and $R_{M3} = 7.2\times10^{-6}$ m; $R_H = 2.615\times10^{-5}$ m; $\varepsilon_0 = 8.854\times10^{-12}$ $C^{-2}J^{-1}m^{-1}$; $\varepsilon_r = 78.5$ $C^{-1}J^{-1}m^{-1}$; $K = 1.04\times10^{8}$ m^{-1}. The surface potential of magnetite was measured at pH=9 was $\phi_M = -18.36$ mV and $\phi_H = -17.21$ mV.

3.3.2. van der Waals interaction energy (V_A)

The van der Waals force interaction energy (V_A) between magnetite and hematite particles can be expressed as:

$$V_A = -\frac{R_M R_H}{6(R_M+R_H)}\left(\frac{A_{132}}{H}\right) \tag{4}$$

where A_{132} is the effective Hamaker constant of the interaction between magnetite and hematite in an aqueous solution, ie. $A_{132} \approx \left(\sqrt{A_{11}}-\sqrt{A_{33}}\right)\left(\sqrt{A_{22}}-\sqrt{A_{33}}\right)$, where A_{11}, A_{22} and A_{33} are Hamaker constants of magnetite, hematite, and DI water in a vacuum, respectively. According to some relevant literature: $A_{22} = 23.2\times10^{-20}$ J and $A_{33} = 4.0\times10^{-20}$ J. Assume that A_{11} of magnetite is equal to A_{22} of

hematite, and then $A_{11} = A_{22} = 23.2 \times 10^{-20}$ J, while $A_{132} \approx \left(\sqrt{A_{11}} - \sqrt{A_{33}}\right)\left(\sqrt{A_{22}} - \sqrt{A_{33}}\right) = 4.3818 \times 10^{-10}$ J

3.3.3. Magnetic energy (V_{MA})

Magnetic or weak magnetic particles in an aqueous solution have a magnetic effect under an external magnetic field. The formula of magnetic effect energy is calculated by the formula given by Svoboda (2004):

$$V_{MA} = -\frac{32\pi^2 R^6 X^2 B_0^2}{9\mu_0 H_0^3} \tag{5}$$

where R and X represent the radius and the volume coefficient of magnetization of particles, respectively; B_0 is the magnetic induction intensity; μ_0 is the vacuum permeability. However, the magnetic effect energy in this test existed without an external magnetic field. Therefore, the magnetic energy (V_{MA}) can be obtained by referring to the calculation method (Luo and Yang, 1997):

$$V_{MA} = -\frac{2V_H \delta_H \chi_H R_M^6 \sigma_0^2}{9(R_M+H)^6} \tag{6}$$

where V_H, δ_H and χ_H are the volume, density and specific magnetization coefficient of hematite, respectively; σ_H is the geomagnetic action coefficient of magnetite. Based on calculations and references from pertinent literature: $\sigma_0 = 1040$ KA/M, $\delta_H = 2.97 \times 10^3$ Kg/m^3, $\chi_H = 5753.7 \times 10^{-8}$ m^3/Kg.

(4) Hydrophobic energy (V_{HA})

Between hydrophobic surfaces, and even the hydrophobic and the hydrophilic surfaces, there exists a special mutual attraction, namely hydrophobic interaction force. For spherical particles with radius R_1 and R_2 respectively, the relationship between hydrophobic attraction and action distance can be calculated as follows:

$$V_{HA} = 2\pi \frac{R_1 R_2}{R_1+R_2} h_0 V_{HA}^0 \exp\left(-\frac{H}{h_0}\right) \tag{7}$$

where h_0 is the attenuation length, 1~10 nm.

The V_{HA}^0 is the hydrophobic interaction energy constant (mJ.m^{-2}), which can be determined by referring to relevant data:

$$V_{HA}^0 = 2\left[\sqrt{r_3^+}\left(\sqrt{r_1^-} + \sqrt{r_2^-} + \sqrt{r_3^-}\right) + \sqrt{r_3^-}\left(\sqrt{r_1^+} + \sqrt{r_2^+} + \sqrt{r_3^+}\right) - \sqrt{r_1^+ r_2^-} - \sqrt{r_1^- r_2^+}\right] \tag{8}$$

where r_1^+, r_2^+, r_3^+ are the electron acceptor components of the surface energy of magnetite, hematite, and DI water respectively; r_1^-, r_2^-, r_3^- are electron donor components of the surface energy of the magnetite, hematite, and DI water respectively.

For water medium, $r_3^+ = r_3^- = 25.5$ mJ/m^2, $r_1^+, r_1^-, r_2^+, r_2^-$ can be obtained by using the following formula:

$$(1 + cos\,\theta) r_L = 2\left(\sqrt{r_S^d r_L^d} + \sqrt{r_S^d r_L^d} + \sqrt{r_S^d r_L^d}\right) \tag{9}$$

where r_L, r_L^d, r_L^+, r_L^- are the surface energy of the liquid, the dispersion component of the surface energy, the electron acceptor component, and the donor component respectively; for water medium, $r_L = 72.8\ \frac{\text{mJ}}{\text{m}^2}, r_L^d = 21.8$ mJ/m^2; r_S^d, r_S^+ and r_S^- are the dispersion component, the electron receiver component, and the donor component of the solid surface energy respectively; θ is the contact angle of liquid and solid surface; for monopolar surfaces, $r_s^+ \approx 0$. The above equation is simplified as:

$$(1 + cos\,\theta) r_L = 2\left(\sqrt{r_s^d r_L^d} + \sqrt{r_s^- r_L^-}\right) \tag{10}$$

and r_s^d can be determined by the following equation: $A = 1.51 \times 10^{-21} r_s^d$

If $V_H > 0$, the repulsive force plays the dominant role, represented by V_{HR}; if $V_H < 0$, that is, the gravitational force becomes vital, represented by V_{HA}. It can be calculated that magnetite $r_S^d = 43.56$ mJ/m^2 and hematite $r_S^d = 153.64$ mJ/m^2, while $V_{HR}^0 = -45.16$ mJ/m^2 and $h_0 = 2.5$ nm.

As shown in Fig. 8, the EDLVO curves of magnetite with different particle sizes and fine hematite particles (-45 μm) at pH=9 could be obtained by combining electrostatic energy, van der Waals interaction energy, magnetic energy, and hydrophobic energy in sodium oleate. The results indicated that fine magnetite and fine hematite had a strong attraction after overcoming the weak barrier.

Therefore, in the sodium oleate system, under the condition of inputting certain mechanical energy, the fine magnetite particles could adhere to the coarse hematite particles or agglomerate with each other to increase the apparent size of hematite particles, which improved the possibility of hematite particles adhering to bubbles and thereby enhanced the flotation recovery of fine hematite particles.

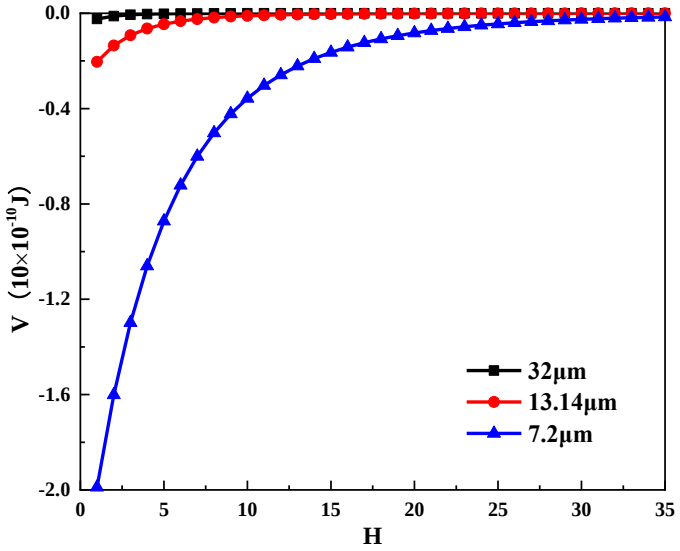

Fig. 8. Total interaction energy curves of magnetite with different particle sizes and fine hematite particles

3.4. Laser particle size analysis

Fig. 9 reveals the particle size distribution of the -45 μm hematite before and after adding magnetite particles with different particle sizes (-106+45 μm and -18 μm) in sodium oleate solution. As shown in Fig. 9, the average size of hematite particles increased from 26.152 μm to 40.686 μm after adding 20% of -18 μm magnetite particles. This indicated that adding -18 μm magnetite particles in sodium oleate solution could agglomerate the hematite particles, increasing the apparent size of hematite particles as well as the probability of adsorbing to bubbles, and therefore, the flotation recovery of hematite was improved. This was consistent with the result that fine magnetite particles could improve the flotation recovery of the fine hematite particles. In addition, it can be seen that the average size of hematite particles increased from 26.152 μm to 369.873 μm after adding 20% of -106+45 μm magnetite particles, and the fine hematite particles almost disappeared. The reason for this phenomenon might be that two kinds of mineral particles could coalesce into coarser particles, and their particle sizes were larger than that the bubbles could carry. Therefore, the floatability was decreased, which confirmed the result that the hematite flotation recovery was decreased after adding the -106+45 μm magnetite particles.

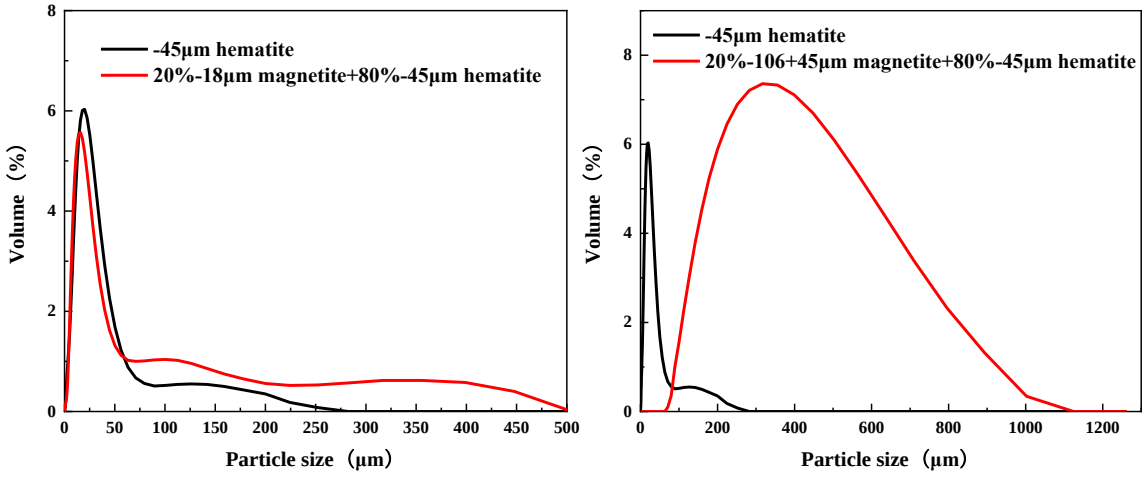

Fig .9. Particle size distribution diagram of -45 μm hematite before and after adding magnetite particles in sodium oleate solution

3.5. Sedimentation tests

The effect of magnetite with different particle sizes on the settlement of fine hematite particles is shown in Fig. 10. The results showed that the sedimentation rate of fine hematite particles increased gradually with increasing the percentage of magnetite particles, which indicated the addition of magnetite could increase the apparent granularity of fine hematite particles. The finer the particle size of magnetite, the faster the sedimentation rate of hematite. The sedimentation rate of hematite increased from 78.3% to 94.6% when the content of the -18 μm magnetite increased from 0% to 20%. This indicated that the finer magnetite particle size, the more obvious the agglomeration effect of hematite.

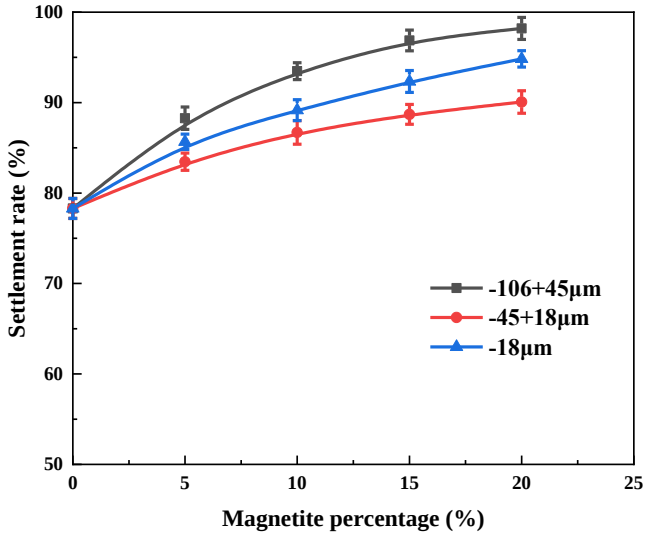

Fig. 10. Effect of magnetite with different particle sizes on the settlement rate of fine hematite particles

4. Conclusions

(1) The addition of magnetite with the same particle sizes as hematite during the direct flotation of -45 μm hematite using sodium oleate as a collector is beneficial to improve the recovery of hematite and the Fe grade of concentrate, but the addition of magnetite with different particle size (-106+45 μm) as hematite will reduce the flotation recovery of hematite (-45 μm). Therefore, the beneficial effect can be achieved by adjusting the particle sizes to avoid the adverse effect.

(2) Microscopic analysis, laser particle size analysis, and EDLVO calculation confirm that there is an effective aggregation between fine magnetite and hematite particles. Thereby, the apparent diameter of hematite is enlarged and the contact probability, as well as the adhesion efficiency between fine particles and bubbles, are increased, thus improving the hematite recovery. Sedimentation tests supplement the conclusion that the aggregation effect of fine hematite is enhanced with the addition of magnetite particles, and the smaller the particle size, the stronger the aggregation effect.

Acknowledgements

The authors gratefully acknowledge the financial support from the National Natural Science Foundation of China (Grant No. 51964025 and 51604130), Ten Thousand Talent Plans for Young Top-notch Talents of Yunnan Province (YNWR-QNBJ-2018-167), and the Fund Project of the Analytic and Testing Research Center of Kunming University of Science and Technology (2020T20140027). Additionally, the authors would like to express our gratitude to editors and reviewers for their diligent work.

References

AHMED, M.A., ALI, S.M., EI-DEK, S., GALAL., A., 2013. *Magnetite–hematite nanoparticles prepared by green methods for heavy metal ions removal from water*. Mater. Sci. Eng. B-Solid State Mater. Adv. Technol, 178, 744-751.

AKINWEKOMI, V., MAREE, J.P., MASINDI, V., ZVINOWANDA, C., OSMAN, M.S., FOTEINIS, S., MPENYANA-MONYATSI L., CHATZISYMEON, E., 2020. *Beneficiation of acid mine drainage (AMD): A viable option for the synthesis of goethite, hematite, magnetite, and gypsum - Gearing towards a circular economy concept*. Miner. Eng. 148, 106204.

BHOWMIK, R.N., SARAVANAN, A., 2010. *Surface magnetism, Morin transition, and magnetic dynamics in antiferromagnetic a-Fe_2O_3 (hematite) nanograins*. J. Appl. Phys. 107, 053916.

BODE, P., MCGRATH, T.D.H., EKSTEEN, J.J., 2020. *Characterising the effect of different modes of particle breakage on coarse gangue rejection for an orogenic gold ore*. Miner. Process. Extr. Metall. 129, 35-48.

CHAPMAN, N.A., SHACKLETON, N.J., MALYSIAK, V., O'CONNOR, C.T., 2011. *The effect of using different comminution procedures on the flotation of Platinum-Group Minerals*. Miner. Eng. 24, 731-736.

DARABI, H., KOLEINI, S.M.J., DEGLON, D., REZAI, B., ABDOLLAHY, M., 2016. *Investigation of bubble-particle attachment, detachment and collection efficiencies in a mechanical flotation cell*. Powder. Technol. 375, 109-123.

FORBES, E., 2011. *Shear selective and temperature responsive flocculation: A comparison of fine particle flotation techniques.* Int. J. Miner Process. 99, 1-10.

FU, Y.F., YIN, W.Z., YANG, B., LI, C, ZHU, Z.L., LI, D., 2018. *Effect of sodium alginate on reverse flotation of hematite and its mechanism*. Int. J. Miner. Metall. Mater. 25, 1113–1122.

GUO, L.X., OU, Z.S., HU, M.X., 1999. *EDLVO theory and its application in coal slurry suspension*. China. Min. Mag. 6, 3-5.

HAO, H.Q., LI, L.X., SOMASUNDARAN, P., YUAN, Z.T., 2019. *Adsorption of pregelatinized starch for selective flocculation and flotation of fine siderite*. Langmuir. 35, 6878-6887.

HASELHUHN, H., KAWATRA, S.K., 2015. *Flocculation and dispersion studies of iron ore using laser scattering particle size analysis.* Miner. Metall. Process. 32, 191-195.

HU, P., LIANG, L., PENG, Y.L., YU, H.S., XIE, G.Y., 2020. *Recovery of microcrystalline graphite from Quartz Using Magnetic Seeding*. Minerals (Basel). 10, 24.

HU, W.T., WANG, H.J., LIU, X.W., WANG, B., 2013. *Monomer dissociation characteristics and selective recovery technology of micro-fine iron particles.* J. Univ. Sci. Technol. B. 35, 1424-1430.

LEJA, J., (1957, 1957). *Mechanism of collector adsorption and dynamic attachmentof particles to air bubbles as derived from surface-chemical studies*. Trans. IMM 66, 425–437 (1956, 1957).

LI, D., YIN, W.Z., LIU, Q, CAO, S.H., SUN, Q.Y., ZHAO, C., YAO, J., 2017. *Interactions between fine and coarse hematite particles in aqueous suspension and their implications for flotation*. Miner. Eng. 114, 74-81.

LI, D, YIN, W.Z., SUN, C.B., ZHANG, R.Y., 2019. *The self-carrier effect of hematite in the flotation.* Chin. J. Eng. 41, 1397-1404.

LI, H., LIU, M., LIU, Q., 2018. *The effect of non-polar oil on fine hematite flocculation and flotation using sodium oleate or hydroxamic acids as a collector*. Miner. Eng. 119, 105-115.

LUO, J.K., YANG, J.L., 1997. *Theoretical criterion for the dispersion and agglomeration of fine mineral particles in a compound force field system.* Met. Ore. Dressing. Abroad. 11, 12-18.

LUO, X.M., YIN, W.Z., SUN, C.Y., WANG, N.L., MA, Y.Q., WANG, Y.F., 2016. *Improved flotation performance of hematite fines using citric acid as a dispersant*. Int. J. Miner. Metall. Mater. 23, 1119-1125.

MA, J.Y., XU, X., XIA, W., FU, K., LIAO, Y., 2019. *Flocculation of a high-turbidity kaolin suspension using hydrophobic modified quaternary ammonium salt polyacrylamide*. Processes. 7, 108.

MEDVEDEVA, I., BAKHTEEVA, Y., ZHAKOV, S., REVVO, A., BYZOV, I., UIMIN, M., YERMAKOV, A., MYSIK, A., 2013. *Sedimentation and aggregation of magnetite nanoparticles in water by a gradient magnetic field,* J. Nanopart. Res. 15, 1-8.

OZKAN, A., DUZYOL, S., 2014. *Gamma processes of shear flocculation, oil agglomeration and liquid–liquid extraction.* Sep. Purif. Technol. 132, 446-451.

PAIVA, M., RUBIO, J., 2016. *Factors affecting the floto-elutriation process efficiency of a copper sulfide mineral*. Miner. Eng. 86, 59-65.

PANDA, L., DAS, B., RAO, D.S., MISHRA, B.K., 2011. *Selective flocculation of banded hematite quartzite (bhq) ores.* Open. Miner. Process. J. 4, 45-51.

PASCOE, R.D., DOHERTY, E., 1997. *Shear flocculation and flotation of hematite using sodium oleate.* Int. J. Miner Process, 51, 269-282.

PINDRED, A., MEECH, J.A., 1984. *Interparticular phenomena in the flotation of hematite fines.* Int. J. Miner. Process. 12, 193-212.

RAO, Z.Q., ZHANG, Y.S., JIN, 2013. *Improved flotation of oolitic hematite ore based on a novel cationic collector*. Appl. Mech. Mater. 303-306, 2713-2716.

ROBINSON, P., HARRISON, R.J., MCENROE, S.A., HARGRAVES, R.B., 2004. *Nature and origin of lamellar magnetism in the hematite-ilmenite series*. Am. Miner. 89, 725-747.

SCHALLER, V., KRALING, U., RUSU, C., PETERSSON, K., WIPENMYR, J., KROZER, A. WAHNSTROM, G., SANZVELASCO, A., ENOKSSON, P., JOHANSSON, C., 2008. *Motion of nanometer sized magnetic particles in a magnetic field gradient*. J. Appl. Phys. 104, 093918.

SVOBODA, J., 2004. *Magnetic Techniques for the Treatment of Materials*. Kluwer Academıc Publıshers.

SYVITSKI, J.P.M., 1991. *Principles, methods, and application of particle size analysis: Contents.* Earth-Sci. Rev. 33, 59-61.

VIEIRA, A.M., PERES, AEC., 2007. *The effect of amine type, pH, and size range in the flotation of quartz*. Miner. Eng. 20, 1008-1013.

WANG, Y., FORSSBERG, E., 1992. *Aggregation between magnetite and hematite ultrafines utilizing remanent magnetization*. Miner. Eng. 5, 895-905.

YANG, Z.J., XU, X.Y., YUAN, X.Y., 2019. *Experimental study on selective flocculation flotation of low-grade tin slime*. China. Min. Mag. 28, 212-215, 219.

YIN, W.Z., WANG, D.H., DRELICH, J.W., YANG, B., LI, D., YAO, J., 2019. *Reverse flotation separation of hematite from quartz assisted with magnetic seeding aggregation*. Miner. Eng. 139, 105873.

YUE, T., WU, X.Q., DAI, L., 2019. *Effect of magnetic seeding agglomeration on flotation of fine minerals.* J. Cent. South Univ. 26, 75-87.

ZHANG, M.J., XU, Q., LUO, J.K., 1986. *Mechanism of aggregation between fine particles of hematite and magnetite*. Nonferrous Met. Eng. 38, 21-26.

ZHUO, Q.M., LIU, W.L., XU, H.X., SUN, X.P., ZHANG, H., LIU, W., 2018. *The effect of collision angle on the collision and adhesion behavior of coal particles and bubbles*. Processes. 6, 218.